2014 International Conference on Unmanned Aircraft Systems (ICUAS)
May 27-30, 2014. Orlando, FL, USA

Linear Parameter Varying Control Synthesis: State Feedback versus $H\infty$ Technique with Application to Quadrotor UAV

Iman Sadeghzadeh, Abbas Chamseddine, Didier Theilliol and Youmin Zhang*

***Abstract*—This paper focuses on the synthesis of Linear Parameter Varying (LPV) control based on two different LPV control structures. In the first structure the $H\infty$ self-Gain-Scheduling (GS) control technique is used to obtain the LPV controller and in the second method, the composite quadratic Lyapunov function and the quadratic cost function are used to find the optimal state feedback gain. Finally, a six-degree of freedom quadrotor helicopter is used as an illustrative plant to compare the results of both LPV control structures.**

I. INTRODUCTION

Aerospace systems have benefited from a variety of modern multivariable feedback control techniques over the past few decades. Most of these controllers are designed based on various operating points of the linearized plant and the gain scheduling technique is used for interpolation between the controller gains for each point. The interpolation process is mainly designed based on parameter variables of the plant. However, these ad-hoc methods are not capable of guaranteeing the stability, performance and the robustness of the controller other than the design points. Therefore, design and application of scheduling multivariable controllers is a complex and time consuming task. To overcome these difficulties, Linear Parameter Varying (LPV) control technique is introduced as an alternative gain scheduling method. As it can be understood from its name, the LPV systems are based on linear structure with a set of varying parameters over time. In other words, the model and the controller are linear but the nonlinear dynamics of the plant and the controller are dependent to certain time-varying parameters. The value of time-varying parameter is based on plant's operational conditions, and can be measured in real time.

I. Sadeghzadeh is with the Department of Mechanical and Industrial Engineering of Concordia University, Montreal, CANADA.
A. Chamseddine is currently with the École de Technologie Supérieure (ÉTS) and formally with Concordia University, Montreal, CANADA.
D. Theilliol is with the Research Centre for Automatic Control of Nancy (CRAN) at University of Lorraine, FRANCE.
Y.M. Zhang is with the Department of Mechanical and Industrial Engineering of Concordia University, Montreal, CANADA. (Corresponding author, e-mail: ymzhang@encs.concordia.ca).

When the plant's dynamics vary over the time based on operating conditions, the appropriately pre-designed controller can be selected based on weighting functions to guarantee the stability, performance, and robustness of the plant.

The LPV systems can be represented in input-output or state-space form and either in continuous or discrete-time. The continuous representation of the LPV system is shown in the following form [1]:

$$\begin{aligned}\dot{x} &= A(\rho(t))x + B(\rho(t))u \\ y &= C(\rho(t))x + D(\rho(t))u\end{aligned} \tag{1}$$

where x and y represent the states and output vectors and u and ρ represent the control input and varying parameter respectively. A general scheme of the controlled LPV system is presented in Fig. 1.

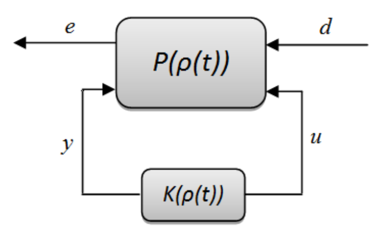

Figure 1. The controlled LPV system

where d is the desired set point and e is the error between the set point and the real output of the plant.

In order to obtain the LPV model from a physical representation of the nonlinear model, three methods can be used: Jacobian linearization, state transformation and substitution function method [2]. The main objective of using these methods is to distribute (hide) the nonlinearity of the system into time-varying parameter. Also one can use the Least Square (LS) or the Recursive Least Square (RLS) methods to obtain the model from experimental data [3]. The objective of this paper is to present two different LPV control structures synthesized based on different techniques and to compare the performance of both control structures using a quadrotor helicopter UAV. This paper is organized as follows:

In Section II, the dynamic model of the quadrotor helicopter which has been used as an illustrative plant including its configuration, geometry, and parts are described. In Section III, the brief description for LPV synthesis using state feedback method is illustrated and has been followed by the synthesis of gain-scheduling $H\infty$ LPV controller in Section IV. Finally the results for both methods are presented and briefly compared in Section V.

II. Dynamic Model of Quadrotor Helicopter

The quadrotor is a helicopter that is lifted and propelled by four rotors. Each rotor is mounted on the end tip of the equal-in-length aluminum arms which are connected to the central body. The front and rear rotors spin clockwise and the left and the right rotors spin counterclockwise. Quadrotor helicopter is considered as an under-actuated system due to its four actuators (rotors) and the six parameters to control (6 DoF). The quadrotor UAV available at the Network Autonomous Vehicle (NAV) Lab in the Department of Mechanical and Industrial Engineering of Concordia University is the Qball-X4 as shown in Fig. 2, which was developed by Quanser Inc. partially under the financial support of NSERC (Natural Sciences and Engineering Research Council of Canada) in association with an NSERC Strategic Project Grant led by Concordia University since 2007.

The quadrotor UAV is enclosed within a protective carbon fiber ball-shape cage (therefore a name of Qball-X4) to ensure safe operation. It uses four 10×4.7 inch propellers and standard RC motors and speed controllers.

The Qball-X4's proprietary design ensures safe operation and opens the possibilities for a variety of novel applications. The protective cage is a crucial feature since this unmanned aerial vehicle was designed mainly for use in an indoor environment/laboratory, where there are typically many close-range hazards (including other vehicles) and personnel doing flight tests with the Qball-X4.

To obtain the measurement from onboard sensors and to drive the motors connected to the four propellers, the Qball-X4 utilizes Quanser's onboard avionics Data Acquisition Card (DAQ), the HiQ, and the embedded Gumstix single-board micro-computer. The HiQ DAQ is a high-resolution Inertial Measurement Unit (IMU) and an avionic Input/Output (I/O) card designed to accommodate a wide variety of applications. QuaRC, Quanser's real-time control software, allows researchers and developers to rapidly develop and test controllers on actual hardware through a MATLAB/Simulink interface. The open-architecture of QuaRC and the extensive Simulink blocksets provide users with powerful control development tools. QuaRC can target the Gumstix embedded computer automatically to generate code and execute controllers onboard the vehicle. During flights, while the controller is executing on the Gumstix, users can tune parameters in real-time and observe sensor measurements from a host ground station computer (PC or laptop).

Figure 2. The Qball-X4 quadrotor UAV (Quanser, 2010)

The entire UAV system's block diagram is illustrated in Fig. 3. It is composed of three main parts. The first part represents the Electronic Speed Controllers (ESCs) + the motors + the propellers in a set of four. The input to this part is $u = [u_1\ u_2\ u_3\ u_4]^T$ which are Pulse-Width Modulation (PWM) signals. The output is the thrust vector $T = [T_1\ T_2\ T_3\ T_4]^T$ generated by four individually-controlled motor-driven propellers. The second part is the geometry that relates the generated thrusts to the applied lift and torques to the system. This geometry corresponds to the position and orientation of the propellers with respect to the center of mass of the Qball-X4. The third part is the dynamics that relate the applied total lift and torques to the position (P), velocity (V) and acceleration (A) of the Qball-X4.

The subsequent sections describe the corresponding mathematical model for each of the blocks of Fig. 3.

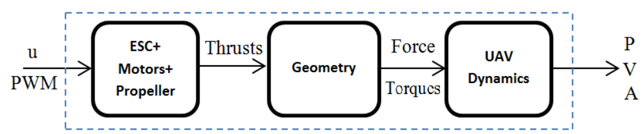

Figure 3. The UAV system block diagram

A. ESCs, Motors and Propellers

The motors of the Qball-X4 are outrunner brushless motors. The generated thrust T_i of the i^{th} motor is related to the i^{th} PWM input u_i by a first-order linear transfer function:

$$T_i = K \frac{\omega}{s+\omega} u_i \tag{2}$$

where $i = 1, ...,4$ and K is a positive gain and ω is the motor bandwidth. K and ω are theoretically the same for the four motors but this may not be the case in practice. It should be noted that $u_i = 0$ corresponds to zero thrust and that $u_i = 0.05$ corresponds to the maximal thrust that can be generated by the i^{th} motor due to physical limitation (saturation limit) of the motor.

B. Geometry

A schematic representation of the Qball-X4 is given in Fig. 4. The motors and propellers are configured in such a way that the back and front (1 and 2) motors spin clockwise and the left and right (3 and 4) spin counterclockwise.

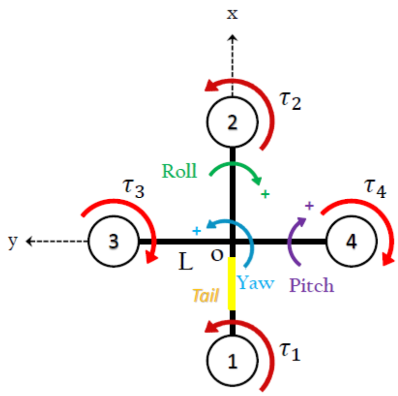

Figure 4. Schematic representation of the Qball-X4

Each motor is located at a distance L from the center of mass o and when spinning, a motor produces a torque τ_i which is in the opposite direction of that motor runs as shown in Fig. 4. The origin of the body-fixed frame is the system's center of mass o with the x-axis pointing from back to front and the y-axis pointing from right to left. The thrust T_i generated by the i^{th} propeller is always pointing upward in the z-direction in parallel to the motor's rotation axis. The thrusts T_i and the torques τ_i result in a lift in the z-direction (body-fixed frame) and torques about the x, y and z axis.

The relation between the lift/torques and the thrusts is:

$$\begin{aligned} u_z &= T_1 + T_2 + T_3 + T_4 \\ u_\theta &= L(T_1 - T_2) \\ u_\phi &= L(T_3 - T_4) \\ u_\varphi &= \tau_1 + \tau_2 - \tau_3 - \tau_4 \end{aligned} \quad (3)$$

The torque τ_i produced by the i^{th} motor is directly related to the thrust T_i via the relation of $\tau_i = K_\psi T_i$ with K_ψ as a constant. In addition, by setting $T_i \approx Ku_i$ from (2), the relation (3) can be re-written as:

$$\begin{bmatrix} u_z \\ u_\theta \\ u_\phi \\ u_\psi \end{bmatrix} = \begin{bmatrix} K & K & K & K \\ KL & -KL & 0 & 0 \\ 0 & 0 & KL & -KL \\ KK_\psi & KK_\psi & -KK_\psi & -KK_\psi \end{bmatrix} \begin{bmatrix} u_1 \\ u_2 \\ u_3 \\ u_4 \end{bmatrix} \quad (4)$$

where u_z is the total lift generated by the four propellers and applied to the quadrotor UAV in the z-direction (body-fixed frame). u_θ, u_φ and u_ψ are respectively the applied torques in θ, φ and ψ directions.

C. UAV Nonlinear Dynamic Model

As mentioned above, the thrust (lift) vectors generated by four motors is $T = [T_1\ T_2\ T_3\ T_4]^T$. Also twelve states are considered for the quadrotor as follows [4]:

$$x = [x\ y\ z\ \dot{x}\ \dot{y}\ \dot{z}\ p\ q\ r\ \phi\ \theta\ \psi]^T \quad (5)$$

Table I contains the nominal values of the quadrotor helicopter's system parameters.

TABLE I. SYSTEM SPECIFICATIONS

M	J_{xx}	J_{yy}	J_{zz}	L	Ω_{motor}
1.4	0.03	0.04	0.04	0.2	15
Kg	Kg.m^2	Kg.m^2	Kg.m^2	m	rad/sec

The dynamic model of the quadrotor can be represented as follows:

$$\begin{aligned} \dot{x} &= f_1(x,u) = \dot{x}; \\ \dot{y} &= f_2(x,u) = \dot{y}; \\ \dot{z} &= f_3(x,u) = \dot{z}; \\ \ddot{x} &= f_4(x,u) = (\sin\psi \sin\phi + \cos\psi \sin\theta \cos\phi)\frac{U_1}{M}; \\ \ddot{y} &= f_5(x,u) = (\sin\psi \sin\theta \cos\phi - \cos\psi \sin\phi)\frac{U_1}{M}; \\ \ddot{z} &= f_6(x,u) = -g + (\cos\theta \cos\phi)\frac{U_1}{M}; \\ \dot{p} &= f_7(x,u) = \frac{J_{yy} - J_{zz}}{J_{xx}} qr - \frac{J_{TP}}{J_{xx}} q\,\Omega + \frac{U_2}{J_{xx}}; \\ \dot{q} &= f_8(x,u) = \frac{J_{zz} - J_{xx}}{J_{yy}} pr + \frac{J_{TP}}{J_{yy}} p\,\Omega + \frac{U_3}{J_{yy}}; \\ \dot{r} &= f_9(x,u) = \frac{J_{xx} - J_{yy}}{J_{zz}} pq + \frac{U_4}{J_{zz}}; \\ \dot{\phi} &= f_{10}(x,u) = p + \sin\phi \tan\theta\, q + \cos\phi \tan\theta\, r; \\ \dot{\theta} &= f_{11}(x,u) = \cos\phi\, q - \sin\phi\, r; \\ \dot{\psi} &= f_{12}(x,u) = \frac{sin\phi}{\cos\theta} q + \frac{\cos\phi}{\cos\theta} r; \end{aligned} \quad (6)$$

where p, q and r are angular rates in body-fixed frames and J_{TP} is the total rotational moment of inertia around the propeller axis. The linearized LPV model can be achieved by applying Jacobian linearization to (6). It should be mentioned that these hovering conditions are employed for linearization.

III. STATE FEEDBACK TECHNIQUE

For the work to be presented in this paper, the yaw angle is defined as time-varying parameter and its range change between [-π, π].

$$\rho(t) = \psi(t), \qquad \forall t > 0 \quad (7)$$

It is expected that the varying parameter (the yaw angle) appears in state matrix after linearization. The general LPV model can be re-written as follows:

$$\dot{x}(t) = A(\rho(t)x(t) + B(u(t) - u^*) \quad (8)$$

where u^* is equal to the total amount of rotor thrusts in hovering flight condition:

$$u^* = \frac{mg}{4}[1 \quad 1 \quad 1 \quad 1]^T \tag{9}$$

By applying the Jacobian linearization, the linearized state and input matrices can be presented as follows:

$$A(\rho(t)) = \begin{bmatrix} 0&0&0&1&0&0&0&0&0&0&0&0 \\ 0&0&0&0&1&0&0&0&0&0&0&0 \\ 0&0&0&0&0&1&0&0&0&0&0&0 \\ 0&0&0&0&0&0&0&0&0&g\sin\psi&g\cos\psi&0 \\ 0&0&0&0&0&0&0&0&0&-g\cos\psi&g\sin\psi&0 \\ 0&0&0&0&0&0&0&0&0&0&0&0 \\ 0&0&0&0&0&0&0&0&0&0&0&0 \\ 0&0&0&0&0&0&0&0&0&0&0&0 \\ 0&0&0&0&0&0&0&0&0&0&0&0 \\ 0&0&0&0&0&0&1&0&0&0&0&0 \\ 0&0&0&0&0&0&0&1&0&0&0&0 \\ 0&0&0&0&0&0&0&0&1&0&0&0 \end{bmatrix} \tag{10}$$

$$B = \begin{bmatrix} 0&0&0&0 \\ 0&0&0&0 \\ 0&0&0&0 \\ 0&0&0&0 \\ 0&0&0&0 \\ 1/M&0&0&0 \\ 0&\frac{1}{J_{xx}}&0&0 \\ 0&0&\frac{1}{J_{yy}}&0 \\ 0&0&0&\frac{1}{J_{zz}} \\ 0&0&0&0 \\ 0&0&0&0 \\ 0&0&0&0 \end{bmatrix} \tag{11}$$

As it can be seen from (10), the state matrix is parameter dependant but nonlinear with respect to the varying parameter i.e. yaw angle. In order to transform the state matrix into a linear affine function, one can introduce the following polytope form.

$$A(\rho(t)) = \sum_{i=1}^{4} \alpha_i(\rho(t))A_i \tag{12}$$

There is an ad-hoc relation between each element of A_i and $A(\rho(t))$. The nonlinear parts are equal to a_1, a_2, a_3 and a_4 for A_1 , A_2, A_3 and A_4 respectively.

$$a_1 = \begin{bmatrix} 1 & -1 \\ 1 & 1 \end{bmatrix} \quad a_2 = \begin{bmatrix} 1 & 1 \\ -1 & 1 \end{bmatrix}$$
$$a_3 = \begin{bmatrix} -1 & -1 \\ 1 & -1 \end{bmatrix} \quad a_4 = \begin{bmatrix} -1 & 1 \\ -1 & -1 \end{bmatrix} \tag{13}$$

The four weighting functions $\alpha_i(\rho(t))$ are calculated as follows:

$$\alpha_1 = (\frac{1+\cos\rho(t)}{2})(\frac{1+\sin\rho(t)}{2}),$$
$$\alpha_2 = (\frac{1+\cos\rho(t)}{2})(\frac{1-\sin\rho(t)}{2}),$$
$$\alpha_3 = (\frac{1-\cos\rho(t)}{2})(\frac{1+\sin\rho(t)}{2}),$$
$$\alpha_4 = (\frac{1-\cos\rho(t)}{2})(\frac{1-\sin\rho(t)}{2}), \tag{14}$$

In order to synthesize the LPV controller based on optimal control method, one can compute a parameter-varying state feedback controller with the standard infinite positive horizon quadratic cost function. However, the composite quadratic Lyapunov function can be used to obtain the non-conservative result. Hereafter, the final goal is to find the optimal feedback gain by solving an optimization problem.

The general LPV system can be represented as follows:

$$\dot{x}(t) = A(\rho(t))x(t) + Bu(t) \tag{15}$$

where

$$A(\rho(t)) = \sum_{i=1}^{N} \rho_i(t)A_i, \quad \rho_i(t) \geq 0,$$
$$\sum_{i=1}^{N} \rho_i(t) = 1 \quad \forall t > 0 \tag{16}$$

And the infinite positive horizon quadratic cost function is illustrated by following equation:

$$J = \int_0^\infty (x^T Q x + u^T R u) dt \tag{17}$$

Also, the composite quadratic Lyapunov function introduced in [4] can be utilized for a set of positive definite matrices. $P_1, \ldots, P_N \in R^{n \times n}$. Let

$$F_i = P_i^{-1}, \quad i \in I[1, N] \tag{18}$$

For vector, define $\gamma \in R^N$

$$F(\gamma) := \sum_{i=1}^{N} \gamma_i F_i, \quad P(\gamma) := F^{-1}(\gamma) \tag{19}$$

and

$$\Gamma = \left\{ \gamma \in R^N : \sum_{i=1}^{N} \gamma_i = 1, \quad \gamma_i \geq 0, i \in I[1, N] \right\} \tag{20}$$

It is obvious that $F(\gamma)$, $P(\gamma) > 0$ for all $\gamma \in \Gamma$ and the composite quadratic function can be defined as:

$$V_c(x) := \min_{\gamma \in \Gamma} x^T P(\gamma) x \tag{21}$$

Based on Theorem 1 in [4], if $\gamma^*(x)$ is considered as an optimal γ such that

$$x^T P(\gamma^*(x)) x = \min_{\gamma \in \Gamma} x^T P(\gamma) x \tag{22}$$

then

$$\frac{\partial V_c}{\partial x} = 2P(\gamma^*(x))x \tag{23}$$

The feedback control u defined as:

$$u = K(\gamma^*(x))x \tag{24}$$

The time derivative of Lyapunov function is obtained as:

$$V_c(x) = 2x^T P(\gamma^*(x))(A\alpha(t) + BK(\gamma^*(x)))x \quad (25)$$

The following optimization problem which is composed in [5] satisfies the Lyapunov conditions and minimizes the cost function in (17).

$$\begin{aligned} &\min_{P(\gamma),K(\gamma)} \quad tr(P(\gamma)) \\ &s.t. \left\{(A(\alpha) + BK(\gamma))^T P(\gamma) + P(\gamma)A(\alpha) + BK(\gamma))\right\} \\ &< -Q - K(\gamma)^T RK(\gamma) \end{aligned} \quad (26)$$

A new matrix V can be defined such that:

$$V(\gamma)=K(\gamma)F(\gamma) \quad (27)$$

By applying Schur compliment, an equivalent optimization problem will be as follows:

$$\begin{aligned} &\max_{F(\gamma),V(\gamma)} \quad tr(F(\gamma)) \\ &s.t. \begin{bmatrix} \{-A(\alpha)F(\gamma) + BL(\gamma) - A(\alpha)F(\gamma) + BL(\gamma)^T\} & * & * \\ F(\gamma) & Q^{-1} & * \\ V(\gamma) & 0 & R^{-1} \end{bmatrix} \end{aligned} \quad (28)$$

By varying the parameters of the system, the above Bilinear Matrix Inequality (BMI) is transformed to Linear Matrix Inequality (LMI) and solved for each instant of α i.e. F and V at each instant of γ. Finally the feedback gain is achieved as follows:

$$K(\gamma) = V(\gamma)F(\gamma)^{-1} \quad (29)$$

IV. Gain Scheduled H∞ Technique

In this section the $H\infty$ self-gain-scheduling control technique is used to obtain the LPV controller. In this method the linearized equation of motion of the quadrotor is also used to synthesize the LPV controller. Unlike the previous method the yaw angle is not playing any role as the varying parameter, but the state matrix is the function of roll and pitch angles. This way of parameter selection, brings broader flight envelop to quadrotor and makes the controller possible to control the forward flight as well. It should be noted that for each time-varying parameter ρ a certain operating range is determined. However, it is very important to define the range for time-varying parameters properly in order not to overload the calculation burden of the controller. On the other hand, increasing the safety margin for quadrotor's maneuverability tightly is coupled with the range selection of the time-varying parameters. The selected range (parameter space) for each of the two time-varying parameters is: [-0.4 0.4], [-0.4 0.4] with discretized sampling grid of 300×300 respectively.

To synthesize the LPV controller (29), the Bounded Real Lemma (BRL) with the notion of quadratic H∞ performance γ is used as the main tool. For a given Linear Time Invariant (LTI) system with state space realization $G(s)=D+C(SI-A)^{-1}B$, the BRL map for a symmetric matrix P and positive scalar γ can be written from [5] and [6] as follows:

$$B^s_{[A,B,C,D]}(P,\gamma) = \begin{pmatrix} A^T P + PA & PB & C^T \\ B^T P & -\gamma I & D^T \\ C & D & -\gamma I \end{pmatrix} \quad (30)$$

Given a closed-loop LPV system having state space matrices $A(\rho)$, $B(\rho)$, $C(\rho)$ and $D(\rho)$, the system has quadratic $H\infty$ performance γ if and only if there exists a single positive definite matrix P such that:

$$\begin{pmatrix} A^T(\rho)P + PA(\rho) & PB(\rho) & C^T(\rho) \\ B^T(\rho)P & -\gamma I & D^T(\rho) \\ C(\rho) & D(\rho) & -\gamma I \end{pmatrix} < 0 \quad (31)$$

is admissible for all values of the parameter vector ρ. Then the Lyapunov function $V(x) = x^T Px$ can be applied to initiate the global (asymptotic) stability and the L_2 gain is bounded by γ between the input and the output with following form:

$$\|y\|_2 < \gamma \|u\|_2 \quad (32)$$

is applicable for all possible trajectories of ρ and the u is control input vector. Therefore, the $H\infty$ performance requires the existence of a fixed quadratic Lyapunov function for the entire operating range [6]. The estimation of the controller is based on solving the LMI presented in (30) by using the concept of affine Polytopic LPV in [7]. Finally, by using the "hinfgs" tool in MATLAB, the LPV controller gain $K(\rho(t))$ can be obtained as follows:

$$K(\rho(t)) = \sum_{i=1}^{5}\sum_{j=1}^{5} \omega_{1,i}\omega_{2,j} \times K_r \quad (33)$$

where

$$K_r = \begin{pmatrix} A_{k_{i,j}} & B_{k_{i,j}} \\ C_{k_{i,j}} & D_{k_{i,j}} \end{pmatrix} \quad (34)$$

and $\omega_{1,i}$, $\omega_{2,j}$ are the two weighting functions for interpolation of LPV controller gains with 100 (5×5) LTI vertices in a polytopic LPV form and the LPV parameter dependent LPV controller is defined as:

$$\begin{aligned} \dot{x}_K &= A(\rho(t))x + B(\rho(t))e \\ u &= C(\rho(t))x + D(\rho(t))e \end{aligned} \quad (35)$$

where u is the control input and e is the error between reference and the real output signals. As it can be seen from

(35), all matrices are parameter dependent and in the gain-scheduling process, both plant and the controller interpolate automatically and updated based on operating conditions. This ensures the stability, performance and the robustness of the system in the defined range of time-varying parameter [6].

V. Simulation Results

In this section the results for both applied methods are presented. For the first method the quadrotor set point is set to [10 10 10 0 0 180] for *X, Y, Z,* φ*,* θ and Ψ respectively. As it can be seen from figures 5 to 10, all six parameters are following the reference very accurately. In each graph the red color line shows the performance of the first applied method (state feedback LPV) and the blue dashed color line shows the gain-scheduling H∞ LPV method.

It should be mentioned that for the second method, the set point for yaw angle is set to zero since the yaw angle is not considered as the time-varying parameter and it can be varied in any selected range.

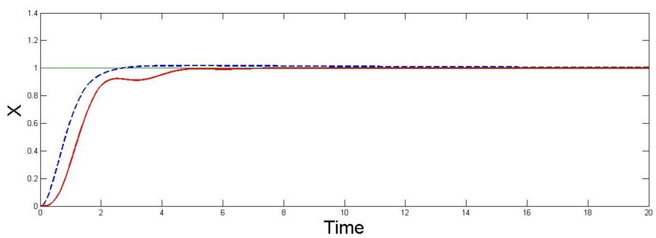

Figure 5. *X* position control

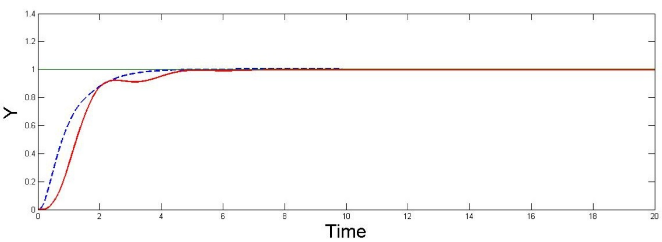

Figure 6. *Y* position control

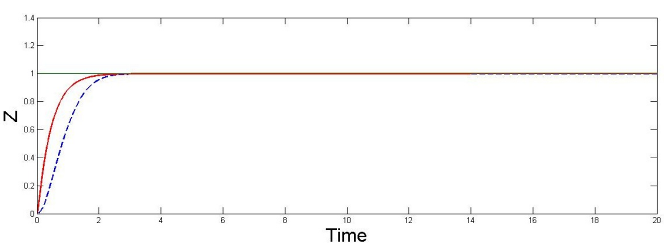

Figure 7. *Z* position control

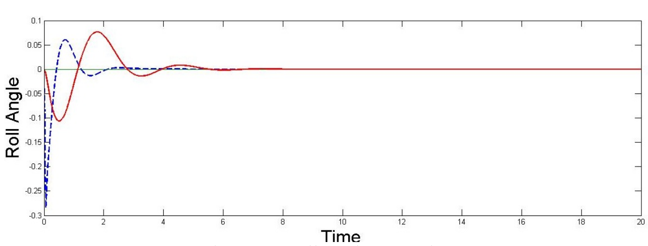

Figure 8. Roll angle control

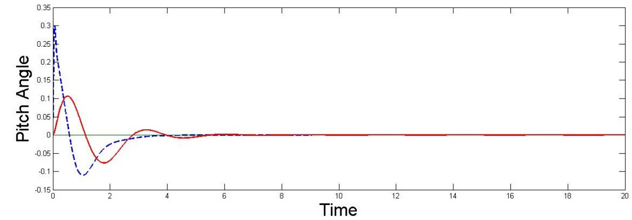

Figure 9. Pitch angle control

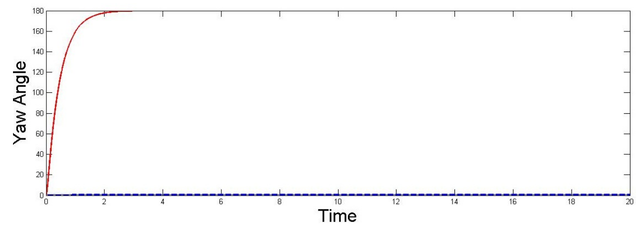

Figure 10. Yaw angle control

VI. Conclusion and Future Work

By comparing the results of both techniques it can be concluded that both controllers are performing very promising for all assigned parameters to be controlled. However, the *H*∞ method showed to be more accurate and robust especially in the control of *X* and *Y* positions. This accurate performance can be due to increased number of LTIs considered in the control synthesis of the LPV controller in comparison to the state feedback optimal control. In other words, since the LTIs (control regions), which shape the vertices of the LPV polytopic hull, help the controller to switch in more accurate manner among the designed local controllers. This design characteristics increases the performance of the quadrotor controller. On the other hand, it should be mentioned that a huge number of LTIs (polytopic vertices) brings a huge burden that can be considered as a drawback to this performance augmentation. The number of LTIs should be in balance with the computation power of the onboard controller.

References

[1] P. Apkarian, P. Gahinet, “A convex characterization of gain-scheduled *H*∞ controllers”, *IEEE Transaction on Automatic Control*, AC-40 (5), 1995, pp. 853-854.

[2] J.S Shamma and J.R Cloutier, “Gain-scheduled missile autopilot design using linear parameter varying transformation” *AIAA Guidance, Control and Dynamics*, vol 16, no. 2, 1998, pp. 256-263.

[3] B. Bamieh & L. Giarré, “LPV models: identification for gain scheduling control,” *European Control Conference*, Porto, Italy.

[4] T. Hu and Z. Lin, “Composite quadratic Lyapunov functions for strained control systems,” *IEEE Transaction on Automatic Control*, vol. 48, no. 3, 2003, pp. 440-450.

[5] A. Serirojanakul and M. Wongsaisuwan, “Optimal control of quad-rotor helicopter using feedback LPV method,” *9th International Conference on Electrical Engineering/Electronics, Computer, Telecommunications and Information Technology*, 2012, pp. 1-4.

[6] P. Apkarian, P. Gahinet, and G. Becker, “Self-scheduled *H*∞ control of linear parameter-varying systems: A design example,” *Automatica*, vol. 31, 1995, pp. 1251-1261.

[7] S.L.M.D. Rangajeeva and J.F. Whidborne, “Linear parameter varying control of a quadrotor,” *6th International Conference on Industrial and Information Systems*, 2011, Seri Lanka.